Research Article

Traumatic brain injury induced by exposure to blast overpressure via ear canal

https://doi.org/10.4103/1673-5374.314311
Date of submission: October 30, 2020
Date of decision: December 22, 2020
Date of acceptance: January 13, 2021
Date of web publication: June 7, 2021

Yang Ou[1, #], Brad A. Clifton[3, #], Jinghui Li[8, #], David Sandlin[3, 4], Na Li[8], Li Wu[8], Chunming Zhang[9], Tianwen Chen[1], Jun Huang[1], Yue Yu[1], Jerome Allison[1], Fan Fan[6], Richard J. Roman[6], James Shaffery[7], Wu Zhou[1, 2], Yi Pang[5, *], Hong Zhu[1, 2, *]

Graphical Abstract *Unprotected ears provide vulnerable loci for blast waves to impact the brain; blast waves delivered into the ear canal cause traumatic brain injury (TBI) which involves chronic neuroinflammation and behavioral deficits*

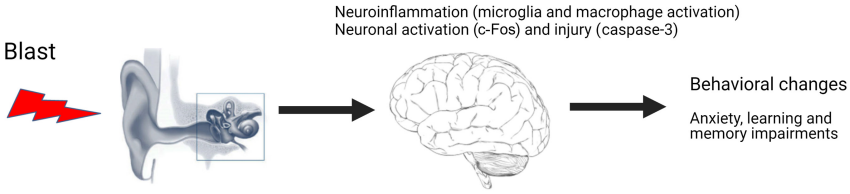

Abstract

Exposure to explosive shockwave often leads to blast-induced traumatic brain injury in military and civilian populations. Unprotected ears are most often damaged following exposure to blasts. Although there is an association between tympanic membrane perforation and TBI in blast exposure victims, little is known about how and to what extent blast energy is transmitted to the central nervous system via the external ear canal. The present study investigated whether exposure to blasts directed through the ear canal causes brain injury in Long-Evans rats. Animals were exposed to a single blast (0–30 pounds per square inch (psi)) through the ear canal, and brain injury was evaluated by histological and behavioral outcomes at multiple time-points. Blast exposure not only caused tympanic membrane perforation but also produced substantial neuropathological changes in the brain, including increased expression of c-Fos, induction of a profound chronic neuroinflammatory response, and apoptosis of neurons. The blast-induced injury was not limited only to the brainstem most proximal to the source of the blast, but also affected the forebrain including the hippocampus, amygdala and the habenula, which are all involved in cognitive functions. Indeed, the animals exhibited long-term neurological deficits, including signs of anxiety in open field tests 2 months following blast exposure, and impaired learning and memory in an 8-arm maze 12 months following blast exposure. These results suggest that the unprotected ear canal provides a locus for blast waves to cause TBI. This study was approved by the Institutional Animal Care and Use Committee at the University of Mississippi Medical Center (Animal protocol# 0932E, approval date: September 30, 2016 and 0932F, approval date: September 27, 2019).

Key Words: anxiety; blast; ear; ear protection; learning; memory; microglia; neuroinflammation; neuron; rat; traumatic brain injury

Chinese Library Classification No. R441; R364; Q2

Introduction

Blast-induced traumatic brain injury (bTBI) has been a major cause of morbidity and mortality in the Iraq and Afghanistan conflicts. In addition to initial injuries, individuals with bTBI are more likely to report long-term consequences, including dizziness and imbalance, anxiety, cognitive deficits, and behavioral deficits (Fausti et al., 2009; Akin and Murnane, 2011; Bogdanova and Verfaellie, 2012; Walker et al., 2015; Muelbl et al., 2018). Primary blast injuries caused by the direct effects of pressure shockwaves on tissues are a source of uncertainty in that they are not always clinically apparent in contrast to a secondary penetrative or tertiary trauma, such as the blunt force trauma after being blown into a wall. The mechanisms that mediate blast wave-induced brain injury remain controversial (Hicks et al., 2010). Proposed mechanisms include direct passage of the blast wave through the skull, in which compression of the torso results in transfer of the blast wave's kinetic energy to the brain via hydraulic oscillations within the vasculature, often associated with intracranial bleeds and subarachnoid hemorrhage (Courtney and Courtney, 2009; Moss et al., 2009; Simard et al., 2014). Another proposed mechanism is that the foramina of the skull such as the acoustic meatus, optic canal, or foramen magnum may provide a conduit for the blast wave to enter the cranial vault (Mediavilla Varas et al., 2011).

As air-filled structures that are directly exposed to the

[1]Departmant of Otolaryngology and Head Neck Surgery, [2]Department of Neurobiology and Anatomical Sciences, [3]MD Program, School of Medicine, [4]Graduate Program in Neuroscience, [5]Department of Pediatrics, [6]Department of Pharmacology and Toxicology, [7]Department of Psychiatry and Human Behavior, University of Mississippi Medical Center, Jackson, MS, USA; [8]Kunming Medical University, Kunming, Yunnan Province, China; [9]Department of Otolaryngology, First Affiliated Hospital, Shanxi Medical University, Taiyuan, Shanxi Province, China

*Correspondence to: Hong Zhu, MD, PhD, hozhu@umc.edu; Yi Pang, MD, PhD, ypang@umc.edu.
https://orcid.org/0000-0002-3944-4624 (Hong Zhu); https://orcid.org/0000-0003-0453-6921 (Yi Pang)
#These authors contributed equally to this work.

Funding: *This study was supported by the National Institutes of Health (NIH) grants R21 DC017293 (to HZ, WZ), R01 DC018919 (to HZ, WZ), AG050049 (to FF), AG057842 (to FF), P20GM104357 (to FF, RJR), and HL138685 (to RJR).*

How to cite this article: *Ou Y, Clifton BA, Li J, Sandlin D, Li N, Wu L, Zhang C, Chen T, Huang J, Yu Y, Allison J, Fan F, Roman RJ, Shaffery J, Zhou W, Pang Y, Zhu H (2022) Traumatic brain injury induced by exposure to blast overpressure via ear canal. Neural Regen Res 17(1):115-121.*

surrounding air, unprotected ears are among the most frequently damaged sites during blast exposure (Dougherty et al., 2013; Ballivet de Régloix et al., 2017). Structures of the external ears serve to collect and direct sound waves into the ear canal, and the middle and inner ears consist largely of air, liquid, and soft tissue with minimal, thin bone separating the cranial vault near the brainstem and the cerebellum. However, the potential contribution of the ear as a conduit of the shock-wave damage to the brain and produce bTBI has not achieved much attention and is controversial. For example, clinical studies of blast victims revealed a significant association between tympanic membrane perforation and loss of consciousness in blast exposure (Xydakis et al., 2007). However, a computational modeling study suggested that changes in intracranial pressure were not associated with changes in pressure in the ear canal (Akula et al., 2015). Therefore, the present study examined whether shock waves directed at the ear is associated with bTBI.

The bTBI animal models in the literature typically use shock tubes that deliver blast waves to the whole head or whole body, in which the orientation of the acoustic meatus with respect to the blast waves is not controlled. Thus, the whole body blast causes damage to not only the brain but also peripheral gas-filled organs such as lungs and intestine. To test the hypothesis that the ears could serve as a route to induce bTBI, we developed a new blast generator that delivers precisely controlled pressure waves directly into the external ear canal (Sandlin et al., 2018; Yu et al., 2020). In the present study, we investigated whether the ear serves as an important conduit for blast exposure-induced brain injury at both structural and functional levels.

Materials and Methods

Animals

Experiments were performed in a total of 79 adult female Long Evans rats weighing 200–250 g (~9–10 weeks old) (Harlan, Indianapolis, IN, USA). This study was conducted in strict accordance with the National Institutes of Health Guide for the Care and Use of Laboratory Animals. The Institutional Animal Care and Use Committee at the University of Mississippi Medical Center approved all the procedures employed in this study (Animal protocol# 0932E, approval date: September 30, 2016 and 0932F, approval date: September 27, 2019). Rats were group housed 2–3 per cage on a 12-hour light/dark cycle in a temperature and humidity-controlled environment, with water and food provided ad libitum.

Blast exposure

To study the role of ear-conducted blast overpressure in the development of TBI while avoiding confounding complications from injuries to additional organ systems, we designed a novel blast generator that delivers focused pressure waves into the external ear canal (Sandlin et al., 2018; Yu et al., 2020). Briefly, a modified high-power air gun outfitted with a high-frequency and high-sensitivity integrated-circuit-piezoelectric (ICP) pressure sensor (PCB Piezotronics, Depew, NY, USA) was attached to a stainless-steel funnel 40 mm in length with a 3.0 mm outlet to direct the pressure pulse to the ear and installed on a stereotaxic frame (David Kopf Instruments, Tujunga, CA, USA). This novel blast generator design produces Friendlander shock waves with a rise time of ~2.2 ms and a duration of ~7.3 ms which resemble the blasts directed at the whole head in previously studies (Cernak et al., 2011; Ewert et al., 2012; Abdul-Muneer et al., 2013; Newman et al., 2015). Blast exposure through the ear canal was performed in isoflurane anesthetized animals (inhalation, 2%, Covetrus, Dublin, OH, USA). Each rat was laid on the right lateral decubitus position. Body temperature was maintained at 37.0°C with a feedback heating pad. Under the guidance of a digital otoscope, the animal's head position was adjusted until the nozzle of the blast generator was centered over the tympanic membrane. The left ear was exposed to a single blast of varying intensities from 0–30 pounds per square inch (psi). Integrity of the tympanic membrane was examined before and after blast exposure. Control animals underwent the same anesthesia, preparation, and monitoring, except the pressure wave was not employed. Following blast exposure, the rats were maintained on a heating pad until fully recovered from anesthesia and continued to be monitored until fully mobile and showing rearing and normal movement.

Immunohistochemistry

Rats were transcardially perfused with saline followed by 4% paraformaldehyde (PFA). Brains were post-fixed in 4% PFA for 24 hours and then cytoprotected sequentially in 10%, 20%, and 30% of sucrose solutions. Serial free-floating coronal sections (40 µm) were prepared using a freezing stage microtome (SM 2000R, Leica, Wetzlar, Germany). To detect and identify cell types that express c-Fos and cleaved caspase-3, double-immunofluorescence staining of c-Fos (1:400, Cat#5348, Cell Signaling Technology, Danvers, MA, USA) or cleaved caspase-3 (Cat# 9664, 1:400; Cell Signaling Technology) with antibodies specific for neurons (NeuN; Cat# MAB377, 1:800; EMD Millipore, Burlington, MA, USA), microglia (Iba1; 1:1000, Cat# 019-19741, FUJIFILM Wako Chemicals USA), and astrocyte (GFAP; Cat#MAB360, 1:1500; EMD Millipore) was performed. To determine if macrophages extravasated into the brain, double-immunofluorescence were performed using antibodies against macrophage marker ED1 (Cat#MAB1435, 1:400; EMD Millipore) and endothelial cell marker CD31 (Cat# PA5-16301, 1:200; Thermo Fisher Scientific, Waltham, MA, USA). Briefly, brain sections were rinsed in PBS twice and blocked with 10% normal goat serum (EMD Millipore) in PBS for 1 hour at room temperature. Following washing in PBS, sections were incubated in primary antibodies overnight at 4°C with gentle shaking. The sections were then washed three times in PBS and incubated with goat anti-mouse-IgG Alex fluo488 (Cat#A28175, 1:400; Thermo Fisher Scientific) or donkey anti-rabbit-IgG (Cat# A32794, 1:1600; Thermo Fisher Scientific) for 2 hours at room temperature. Following washing three times in PBS, the sections were mounted on slides and air-dried. Nuclei were counterstained with DAPI in the mounting medium (Vector Laboratory, Inc. Burlingame, CA, USA). Slides were examined by a confocal laser scanning microscope (Nikon Instruments, Melville, NY, USA) and images were acquired by a digital monochrome camera.

Immunopositive cells were quantified by two approaches. Because Iba$^+$ microglia were brightly immunostained with high density and relative homogenous distribution, they were counted using ImageJ software (version 1.51s, NIH, Bethesda, MD, USA). Briefly, whole brainstem sections (bregma –13 mm) were first scanned using a 10× objective lens to visualize microglia distribution, and then image stacks were acquired using a 20× objective lens in the area indicated by an arrow in **Figure 1B**, where a significant increase of microglia around facial nerve track is observed. The Z-stacks were compressed into a single image, which was converted into 8-bit format. After adjusting the threshold to make individual Iba1$^+$ cells clearly distinguishable from background, the cells were then automatically counted by the software. Cell density was expressed as number of counts per mm^2. Because c-Fos and caspase-3$^+$ cells were much less abundant with highly heterogeneous distribution, they were counted manually under 20× objective lens. c-Fos$^+$ cells were counted exhaustively throughout the entire cross section of brainstem (bregma –13 mm) and the regions in hippocampus, habenula and amygdala (bregma –3.9 mm) as illustrated in **Figure 2C**. Caspase-3$^+$ cells were identified only in the brainstem but not any forebrain regions, therefore they were counted only in the brainstem sections. The expression of c-Fos and caspase-3$^+$ cells was presented as total number of positive neurons in

brainstem, hippocampus, amygdala and habenula. A total of 3 sections per rat and 3–9 rats per experimental group were used for histological analysis.

Behavioral tests

Locomotor activity and anxiety behavior were assessed using an open field test (Seibenhener and Wooten, 2015) at 2 and 4 months post blast exposure (sham or 30 psi). The rats were allowed to acclimate in the behavioral test room for 2 hours before the test. Each animal was placed in a 40 × 40 cm activity chamber and allowed 20 minutes to explore. An Opto-Varimex ATM3 Auto-Track System (Columbus Instruments, Columbus, OH, USA) was used to record frequency of entries in each of the monitor's 16 squares defined by infrared beams. The squares were pre-determined to be centrally or peripherally located. The automated software integrated into the ATM3 Auto-Track System counted the beam breaks and duration of time spent in each square. Entries to the central squares and to the total field were analyzed.

An 8-arm water radial maze test (Penley et al., 2013) was performed 12 months after blast exposure to assess the effects on spatial learning and memory. The 8-arm maze was placed in a plastic tub with ~165 cm in diameter and 30 cm in depth. The tub was filled with room temperature water. A labeled escape platform was placed 1 cm below the water surface, at the end of one of the 8 arms. Blast-treated rats and age-matched sham control rats were trained to identify the location of an escape platform marked with a visual cue in one of the 8 arms. Three memory tests were performed 2, 24, and 48 hours after the training. Each test consisted of 5 consecutive trials. Latency to reach the platform was recorded. Data were collected by individuals blinded to the conditions.

Statistical analysis

Statistical analyses were performed using SigmaPlot (Systat Software, Inc., San Jose, CA, USA). Differences among experimental groups were analyzed by two-way analysis of variance (ANOVA) or non-parametric Kruskal-Wallis ANOVA on ranks and *post hoc* Dunn's test. Differences between two experimental groups were analyzed by Student's *t*-test. *P* values of less than 0.05 were considered statistically significant. Mean values ± SEM or the median, quartile (25% and 75%), maximum and minimum are presented.

Results

Post-blast observations revealed a complete recovery of the animals. The animals did not show any signs of severe TBI, i.e., loss of consciousness, loss of balance, loss of coordination, or significant decrease of body weight. The threshold for rupturing the rat tympanic membrane was 15 psi, which is comparable to other animal models of TBI using shock tubes (Ewert et al., 2012; Cho et al., 2013).

Ear blast exposure increases c-Fos expression

Since induction of c-Fos expression is one of the most sensitive indications of neuronal activation upon various insults to the CNS, c-Fos immunofluorescence staining was conducted to determine regional distribution of activated neurons in response to blast exposure. A number of studies have shown that c-Fos induction occurs early in TBI models, typically within 1–6 hours upon insults (Czigner et al., 2004; Wang et al., 2014), therefore we collected brain tissue 1 hour after blast exposure. Exposure to the pressure shockwaves induced an intensity-dependent increase in c-Fos expression in the brainstem around the 4th ventricle and facial nerves (**Figure 2**). Co-staining of the sections with various markers demonstrated that c-Fos were exclusively expressed by NeuN$^+$ neurons (**Figure 2B**) but not GFAP+ astrocytes or Iba$^+$ microglia (data not shown). Although the majority of c-Fos$^+$ neurons were observed in the brainstem (Kruskal-Wallis one way ANOVA on ranks with *post hoc* Dunn's test, H = 10.803 with 3 degrees of freedom, P =0.013), a lesser but significant increase was also detected in certain forebrain regions, including the hippocampus (H = 13.008 with 3 degrees of freedom, P = 0.005), amygdala (H = 18.238 with 3 degrees of freedom, P < 0.001), and habenula (H = 8.519 with 3 degrees of freedom, P = 0.036; **Figure 2D**). There was no significant difference in c-Fos expression between the contralateral and ipsilateral sides of the brain.

Ear blast exposure activates microglia

Reactivity of microglia was examined at 6 hours, 7, 14, 29, and 56 days following 30 psi of ear blast exposure. Ear blast exposure resulted in a marked increase of Iba1$^+$ microglial density in the brainstem (**Figure 1A–H**). Although microglia was activated globally, the blast side especially the region surrounding the facial nerve showed the highest microglial density. Blast-induced microglia activation was also evident by their noticeable morphological transformation. Microglia of control rats exhibited typical ramified morphology characterized with smaller soma and multiple thin and long processes (**Figure 1C**). In contrast, microglia in the blast rats exhibited larger soma but fewer, shorter, and thicker processes (**Figure 1D–H**). The increases in microglial density and morphological transformation were apparent as early as 6 hours post-blast exposure, peaked around 7–14 days, and gradually declined but persisted chronically for up to 56 days. Two-way ANOVA analysis of microglial density in areas surrounding the facial nerve revealed significant effects of blast exposure (P < 0.001), side of blast (P < 0.001), and their interactions (P < 0.001; **Figure 1Q**). Blast exposure induced a significant increase in Iba1$^+$ microglial density on the ipsilateral side of the blast source at all time-points examined, i.e., 6 hours, 7, 14, 29, and 56 days following the exposure. At the peak, i.e., 14 days post blast, blast exposure caused an approximately two-fold increase in microglial density (163.37 ± 8.11 *vs*. 308.69 ± 10.24 counts/mm^2, P < 0.001). On the contralateral side, however, increase in Iba1$^+$ microglial density was only detected at 6 hours and 29 days following the exposure. The density of Iba1$^+$ microglia on the ipsilateral side was significantly higher than those on the contralateral side at 6 hours (P < 0.001), 7 days (P < 0.001), 14 days (P < 0.001), 29 days (P < 0.001), and 56 days (P < 0.001) following blast exposure. There was no significant difference in microglia density between the two sides in sham control rats (P = 0.075).

In addition to the brainstem that showed robust microglial activation, the forebrain regions were also affected. For example, Iba1$^+$ cells in the periventricular region and the hippocampus also exhibited morphologic evidence of activation (**Figure 1I–P**). However, no significant changes in Iba1$^+$ microglial density were observed in either the hippocampus or periventricular areas following blast exposure.

Ear blast exposure leads to macrophage infiltration into the brainstem

To investigate the blood-brain barrier (BBB) integrity following blast exposure, we examined whether blast exposure causes macrophage infiltration by ED1 immunostaining. As expected, ED1$^+$ cells were observed exclusively in the meninges but none in the brain parenchyma of the sham rats. Following 30 psi of ear blast exposure, however, a large amount of ED1$^+$ cells were found in the brainstem parenchyma in a spatiotemporal pattern. For example, a small number of ED1$^+$ cells was noted in the parenchyma at 7 days but not at 6 hours. By day 14, a large amount of ED1$^+$ cells emerged in the parenchyma, primarily located on the medial and ventral domains of the brainstem (**Figure 3**). From day 14 onwards, the number of ED1$^+$ cells tended to decline and were significantly decreased by day 56. To find out if these parenchymal ED1$^+$ cells were infiltrated macrophages from systemic circulation, we performed double-

immunostaining of ED1 with CD31, a marker for endothelial cells. As shown in **Figure 3I–L**, some of the ED1$^+$ cells were apparently in close proximate with blood vessels (arrows in **Figure 3L**), suggesting that they were likely extravasated macrophages due to increased permeability of BBB following blast injury. We did not observe any ED1$^+$ cells in the forebrain areas.

Ear blast exposure induces neuronal injury

Following 30 psi blast exposure there was a significant increase of caspase-3$^+$ cells in the brainstem (**Figure 4A**). Double-immunostaining revealed that caspase-3 expressing cells were exclusively NeuN$^+$ neurons (**Figure 4B**). Interestingly, activation of caspase-3 seemed to be a delayed event as it was not observed at earlier time-points (6 or 24 hours post-blast). Quantitative analysis revealed a significant increase in caspase-3$^+$ neurons at 3, 29 and 56 days post blast (Kruskal-Wallis one-way ANOVA on ranks and *post hoc* Dunn's test, $P < 0.001$; **Figure 4C**). We did not observe caspase-3$^+$ cells in the forebrain at any of the time-points examined in the rats exposed to the blast.

Behavioral changes

We examined anxiety behavior of sham ($n = 10$) and blast-exposed rats (30 psi) ($n = 14$) using the open field test. Animals exposed to the blast had fewer entries in the center of the open field than the sham animals at 2 months ($n = 4$, Kruskal-Wallis one way ANOVA on Ranks, $P = 0.005$) following the exposure (**Figure 5**), indicating higher levels of anxiety. There was no difference, however, in number of entries to the total open field (one-way ANOVA on Ranks, $P = 0.12$) suggesting that the effects of blast exposure on the center entry was not due to a general loss in locomotion. At 4 months ($n = 10$) post blast exposure, there was no difference in the number of center entries and total entries.

Eight-arm water maze tests were performed 12 months after the blast exposure. The animals exposed to blast ($n = 11$) took longer time to find the escape platform than the age-matched sham rats ($n = 10$) 2 hours after the training (Student's t-test, $P = 0.034$), indicating impaired learning and memory (**Figure 6**). There was no significant difference in the escape latency between the two groups 24 and 48 hours after the training.

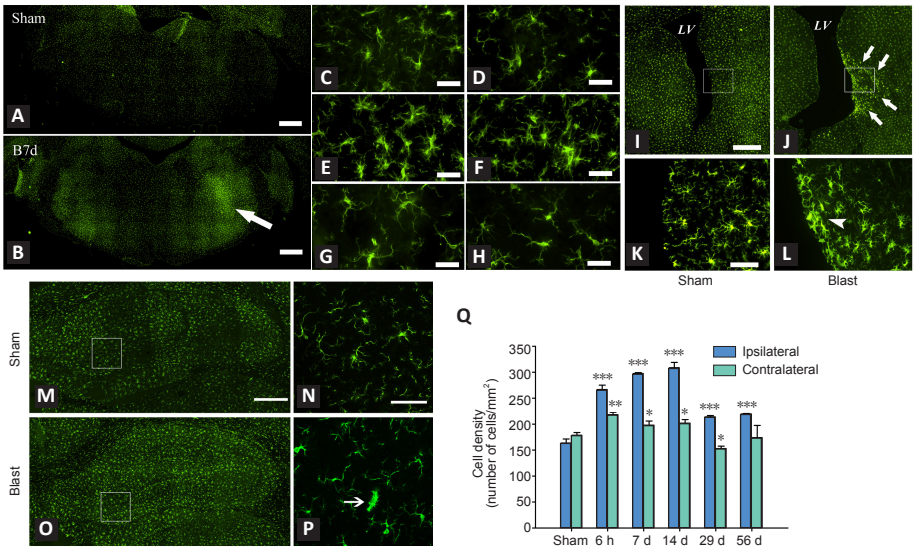

Figure 1 | Ear blast exposure leads to microglial activation.
Representative low power micrographs show a marked increase of Iba1$^+$ microglia across the whole brainstem section in a rat exposed to 30 psi blast (B) as compared to a sham-blast rat (A). The region with highest density of Iba1$^+$ microglia was noted around the facial nerve in the ipsilateral blast side (arrow in B). Microglial transformation from ramified (C: sham) to activated morphology (D–H: 6 hours, 7, 14, 29 and 56 days after blast, respectively) is indicated by their larger cell bodies and thicker/shorter processes. Seven days after blast, activated microglia were also found in the forebrain. The severely affected regions include the lateral ventricle wall adjacent to the caudate putamen, where clusters of activated microglia (denoted by arrows heads and arrow in J & L) were easily found when compared to the sham (I & K). Increased microglial density (O: illustrated by a low power micrograph) and activated characteristics (arrow in P) were also noted in the hippocampus of blasted rats, as compared to the sham rats (M & N). Images N&P were taken from the boxed areas in M and O, respectively. Scale bars: 250 µm in A, B, I, J, M, O and 50 µm in C–H, K, L, N, P. Time-dependent changes of Iba1$^+$ microglia density in the brainstem following blast exposure (30 psi) are shown in Q. Two-way analysis of variance. *$P < 0.05$, **$P < 0.01$, ***$P < 0.001$, *vs.* sham group. $N = 3$–6 each group. LV: Lateral ventricle; psi: pounds per square inch.

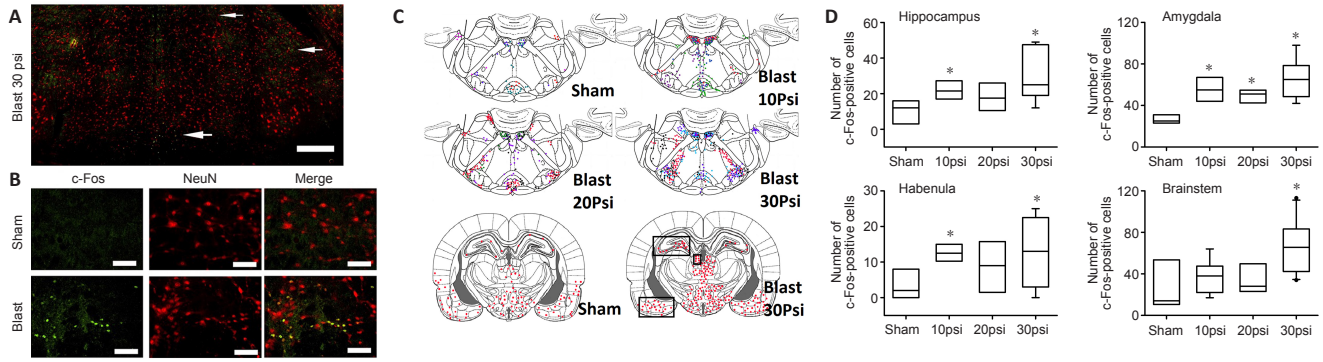

Figure 2 | Blast through the ear induces neuronal c-Fos expression.
Widespread and unevenly distributed c-Fos$^+$ cells (arrows) were detected in the brainstem 1 hour following 30 psi blast (A). Double immunofluorescence showed that c-Fos$^+$ cells were exclusively co-localization with NeuN$^+$ neurons (B). Scale bars: 100 µm in A, 50 µm in B. The distribution of c-Fos$^+$ cells in the brainstem (top and middle panels) and forebrain (bottom panel) is illustrated in C. (D) Quantitative analysis of cell counting showed a significant increase of c-Fos$^+$ cells across different brain regions. Data were analyzed by Kruskal-Wallis one-way analysis of variance on ranks and *post hoc* Dunn's test, each symbol represents the median and quartile (25 and 75%). $N = 7$–9 rats per condition.*$P < 0.05$, *vs.* Sham. psi: Pounds per square inch.

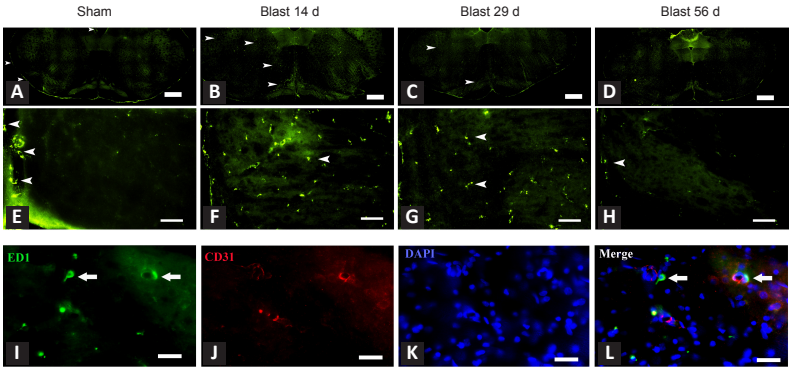

Figure 3 | Infiltration of macrophages in the brainstem after blast exposure.
ED1$^+$ cells (arrow heads) were observed exclusively in the meninges but not parenchyma of sham rats (A & E), whereas a significant number of ED1$^+$ cells emerged in the parenchyma at 14 (B & F) and 29 days (C & G) after blast. By day 56, the number of parenchyma ED1$^+$ cells was markedly reduced. Double-immunostaining revealed that some ED1$^+$ macrophages are closely associated with CD31$^+$ endothelial cells (arrows). Scale bars: 500 µm in A–D, 100 µm in E–H, 50 µm in I–L.

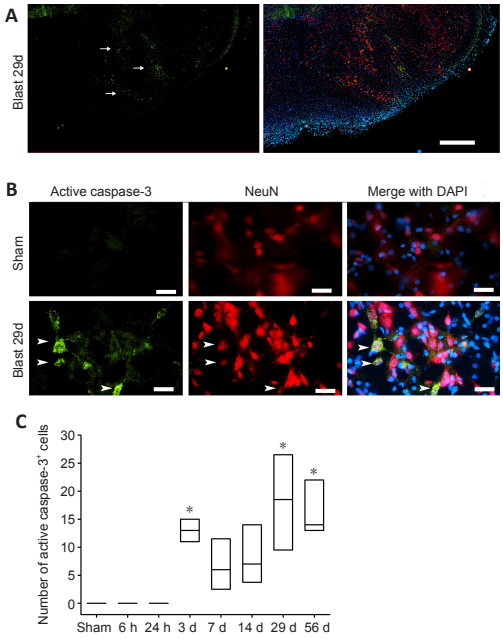

Figure 4 | Activation of caspase-3 by blast exposure (30 psi).
Caspase-3$^+$ cells were detected in the brainstem at 3, 7, 14, 29 and 56 days after blast. Representative low power micrographs indicate clusters of caspase-3$^+$ cells (arrows in A) from a rat 29 days following blast exposure. Double immunostaining revealed that cleaved caspase-3$^+$ cells are exclusively NeuN$^+$ neurons (arrow heads in B). Scale bars: 500 µm in A and 20 µm in B. (C) Analysis of caspase-3$^+$ cell counting. Kruskal-Wallis one-way analysis of variance on ranks, each symbol represents the median, quartile (25% and 75%), n = 4–6 rats per condition. *P < 0.05, *vs.* sham group. psi: Pounds per square inch.

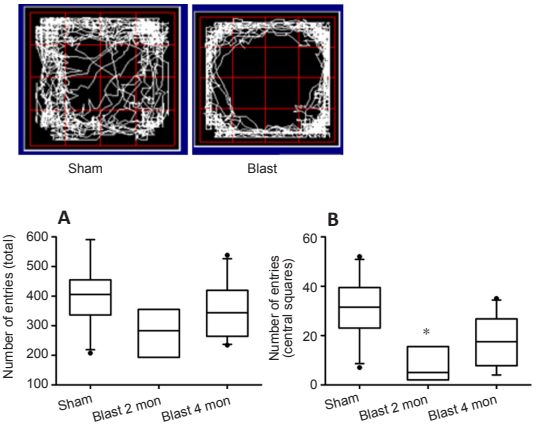

Figure 5 | Animals exhibited signs of anxiety following ear blast exposure.
Open field tests were performed 2 and 4 months following 30 psi of ear blast exposure. Top panel: Representative tracks for sham or blast-exposed rats. The sham rat explored the entire field while the blast-exposed rat avoided open area. Lower Panel: Quantitative analysis revealed that the frequency of entries into the central squares significantly decreased in rats exposed to blast. Kruskal-Wallis one-way analysis of variance on ranks, each symbol represents the median, quartile (25% and 75%), n = 4–10 rats per condition. *P < 0.05, *vs.* sham group. psi: Pounds per square inch.

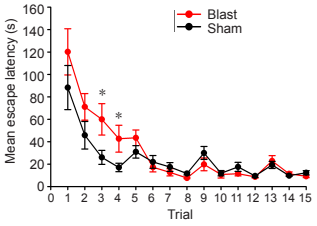

Figure 6 | Ear blast leads to impaired learning and memory in 8-arm maze tests.
Blasted rats (30 psi) exhibited longer escape latency for short-term memory (2 hours post training) at 12 months post blast as compared to age-matched sham controls (Student's t-tests). Trials 1–5: 2 hours post training; trials 6–10: 24 hours post training; trials 11-15: 48 hours post training.*P < 0.05, *vs.* sham group. N = 11 (Blast) and 10 (Sham). psi: Pounds per square inch.

Discussion

The existing animal models of bTBI usually use open field explosion or shock tubes to deliver blast waves to the whole head or whole body (Ma et al., 2019; Kim et al., 2020). To specifically assess the impact of pressure waves through the ear on the brain, our system was designed to address two sources of variance. One is that orientation of the ear canal with respect to the blast waves was fixed in our model. The other one is that the model avoids blast-induced damage to other gas-filled organs such as lungs and intestines. The blast generator in the present study reliably produces a signature Friedlander wave ranging from 0 to 100 psi, with a rise time of 2.2 ms and a duration of 7.3 ms (Sandlin et al., 2018), similar to those generated by an explosion in an open space (Cernak et al., 2011; Ewert et al., 2012). Calibrations show excellent input and output correlations, indicating that the mechanical forces are reproducible and under precise control. The tip of a speculum was aimed to the rat ear canal under the guidance of an otoscope so that the spatial relationship between the direction of the blast wave and the orientation of the ear canal is consistent from blast to blast. The threshold of rupturing the rat tympanic membrane was ~15 psi, which was comparable to other animal studies (Ewert et al., 2012; Cho et al., 2013). The model was validated by our previous studies, which showed that blast exposure evoked well-defined cardiovascular and respiratory responses as well as inner ear vestibular injury in rats (Sandlin et al., 2018; Yu et al., 2020).

Blast victims often experienced ear injuries. Tympanic membrane rupture, hearing loss (Cho et al., 2013), vestibular symptoms such as dizziness and imbalance occurred immediately after blast exposure and some of the symptoms persisted months, or even years after the exposure (Fausti et al., 2009; Akin and Murnane, 2011). The current U.S. army helmet uses layers of Kevlar and a foam suspension to

protect the skull from penetrating and blunt-force injuries, but leaves the ears vulnerable to high-pressure waves from an explosion. Ear protection is often foregone in order to maintain greater situational awareness. A clinical study of 501 US service members (Dougherty et al., 2018) showed that hearing protection was associated with a lower incidence of non-impact, blast wave-induced concussion, suggesting that ears might serve as a direct route of transfer of blast energy to focal areas of the brain. The present study, for the first time, demonstrated that blast waves delivered directly into the external ear canal not only caused peripheral inner ear vestibular damage (Yu et al., 2020), but also caused substantial neurophathological changes in the brain especially in the brainstem near the internal auditory meatus. The transmitted energy of the shockwave was also transmitted to more distant areas of the brain as increased expression of c-Fos was found not only in the brainstem that is closer to the blast source, but also in forebrain regions relevant to cognitive function, anxiety and depression such as the hippocampus, the amygdala and the habenula (Yang et al., 2018). c-Fos is a well-studied immediate-early gene that is used as a marker of neuronal activation in the brain. Increased expression of c-Fos has been associated with several TBI models and considered as an important interface between the primary phase and later pathological manifestations in TBI (Marciano et al., 2002; Russell et al., 2018). The finding of widespread c-Fos activation indicates that the unprotected ear provides a vulnerable locus for blast waves to impact the brain. It is noteworthy that the region surrounding facial nerves showed particular high density of c-Fos expression. A potential means by which transduction may occur is that blast energy from the ear canal ruptures the tympanic membrane, the oval and round windows, then propagates to the brain through the internal auditory meatus which provides a passage through which the vestibulocochlear nerves, the facial nerve, and the labyrinthine artery pass from the inner ear to the brain. This mechanism is supported by a shock tube study conducted with a spherical gelatin filled skull-brain surrogate (Mediavilla Varas et al., 2011). Compared to a closed skull, the presence of openings on the skull and its orientation has a stronger effect on the internal pressure.

A common feature of TBI-induced neuropathology is neuroinflammation (Donat et al., 2017; Simon et al., 2017; Rusiecki et al., 2020). In the current study, we investigated the spatiotemporal changes of microglia after the ear focused blast exposure. Our data demonstrated that the primary mechanical insult by the blast shockwave also triggered a widespread and chronic neuroinflammatory response that was associated with neuronal death and behavioral deficits. Increase in microglial number and morphological changes occurred as early as 6 hours post blast exposure and persisted chronically for up to 56 days, which was companied by neuronal death (caspase-3). Interestingly, the emergence of $ED1^+$ cells exhibited a similar but more delayed pattern that appeared most prominent between days 14 to 29 but largely resolved at day 56 post-blast. The finding that some of the $ED1^+$ cells were in a close proximity of blood vessels suggests that they were likely extravagated macrophages due to increased permeability of the BBB. However, unlike activated Iba^+ microglia found in both the brainstem and forebrain, $ED1^+$ cells were only observed in the brainstem. Together, the results indicate that microglia were activated early and more widespread than macrophages, which were more restricted to the brainstem that is most proximal to the source of the blast.

Brain inflammation appears to have a dual function, i.e. it plays a neuroprotective role during an acute-phase response but becomes detrimental if it persists into a chronic state (Guzman-Martinez et al., 2019; Wofford et al., 2019; Leng and Edison, 2020). The activation of microglia has a significant implication in the development and progression of many neurodegenerative diseases. It has been hypothesized that microglia play dual role in Alzheimer's disease (AD) progression (Hansen et al., 2018; Kinney et al., 2018; Bartels et al., 2020). Early in AD pathogenesis, microglia are essential for clearing Aβ and restoration of homeostasis in the brain. However, prolonged activation of the immune response results in an exacerbation of AD pathology. As the disease progresses, microglia produce proinflammatory factors and lose their ability to clear Aβ. This inflammatory environment ultimately becomes toxic to the surrounding neurons, resulting in neuronal degeneration and disease progression. Blast-induced TBIs are associated with chronic traumatic encephalopathy that may lead to development of AD (Agoston et al., 2017). Studies of military personnel have shown that among TBI subjects exposed to blast, blood Aβ levels were significantly higher than those of non-exposed controls (Olivera et al., 2015). Moderate blast exposure caused a higher concentration of amyloid precursor protein in peripheral blood (Gill et al., 2017). Individuals with bTBI are more likely to report behavioral deficits in mood, anxiety, and negative effects on cognition (Bogdanova and Verfaellie, 2012; Muelbl et al., 2018). The behavioral tests from the current animal study also demonstrated that the animals received ear blast exposure exhibited increased anxiety behavior and impaired learning and memory. Our overall results suggested that unprotected ears provide a vulnerable locus for blast waves to damage the brain; shock waves primarily delivered through the ear canal trigger an acute and chronic inflammatory response that could increase the risk of later development of neurodegenerative diseases such as AD. This vulnerability highlights the necessity for wearing ear protection in blast-prone locations, such as battlefield, training or industrial environments, not only to protect hearing, but also to protect from ear-conducted bTBI. These data further reinforce the importance of development of advanced ear protection that would allow users with normal or enhanced hearing acuity and localization while still protecting the brain from the blast shockwaves via the ear canal and acoustic meatuses.

In conclusion, utilizing an unique ear focused animal model of bTBI, we demonstrated that ear blast caused a substantial neuropathological changes and behavioral deficits in animals, suggesting that the ear provides an important conduit for blast to impact the brain. To better understand the role of the ear in the bTBI, future studies will further investigate whether whole body blast with ear protection can prevent or lower injury severity of bTBI.

Acknowledgments: *We thank UMMC Animal Behavior Core Facility for their excellent technical support in behavioral tests.*
Author contributions: *HZ, WZ and YP designed the research; YO, JL, BAC, DS, NL, LW, CZ, TW, JH, YY, JA, YP, HZ and WZ generated the blast animal model, performed immunohistochemistry staining or data analysis. YO, JS, and TC performed open field tests and data analysis. TC, FF, and RJR performed swim test or data analysis. HZ, YP, WZ, RJR and BAC wrote the paper. All authors approved the final version of this paper.*
Conflicts of interest: *None.*
Financial support: *This study was supported by the National Institutes of Health (NIH) grants R21 DC017293 (to HZ, WZ), R01 DC018919 (to HZ, WZ), AG050049 (to FF), AG057842 (to FF), P20GM104357 (to FF, RJR), and HL138685 (to RJR).*
Institutional review board statement: *All animal procedures were approved by the Institutional Animal Care and Use Committee at the University of Mississippi Medical Center (Animal protocol# 0932E, approval date: September 30, 2016 and 0932F, approval date: September 27, 2019).*
Copyright license agreement: *The Copyright License Agreement has been signed by all authors before publication.*
Data sharing statement: *Datasets analyzed during the current study are available from the corresponding author on reasonable request.*
Plagiarism check: *Checked twice by iThenticate.*
Peer review: *Externally peer reviewed.*

References

Abdul-Muneer PM, Schuetz H, Wang F, Skotak M, Jones J, Gorantla S, Zimmerman MC, Chandra N, Haorah J (2013) Induction of oxidative and nitrosative damage leads to cerebrovascular inflammation in an animal model of mild traumatic brain injury induced by primary blast. Free Radic Biol Med 60:282-291.

Agoston DV, Shutes-David A, Peskind ER (2017) Biofluid biomarkers of traumatic brain injury. Brain Inj 31:1195-1203.

Akin FW, Murnane OD (2011) Head injury and blast exposure: vestibular consequences. Otolaryngol Clin North Am 44:323-334, viii.

Akula P, Hua Y, Gu L (2015) Blast-induced mild traumatic brain injury through ear canal: A finite element study. Biomed Eng Lett 5:281-288.

Ballivet de Régloix S, Crambert A, Maurin O, Lisan Q, Marty S, Pons Y (2017) Blast injury of the ear by massive explosion: a review of 41 cases. J R Army Med Corps 163:333-338.

Bartels T, De Schepper S, Hong S (2020) Microglia modulate neurodegeneration in Alzheimer's and Parkinson's diseases. Science 370:66-69.

Bogdanova Y, Verfaellie M (2012) Cognitive sequelae of blast-induced traumatic brain injury: recovery and rehabilitation. Neuropsychol Rev 22:4-20.

Cernak I, Merkle AC, Koliatsos VE, Bilik JM, Luong QT, Mahota TM, Xu L, Slack N, Windle D, Ahmed FA (2011) The pathobiology of blast injuries and blast-induced neurotrauma as identified using a new experimental model of injury in mice. Neurobiol Dis 41:538-551.

Cho SI, Gao SS, Xia A, Wang R, Salles FT, Raphael PD, Abaya H, Wachtel J, Baek J, Jacobs D, Rasband MN, Oghalai JS (2013) Mechanisms of hearing loss after blast injury to the ear. PLoS One 8:e67618.

Courtney AC, Courtney MW (2009) A thoracic mechanism of mild traumatic brain injury due to blast pressure waves. Med Hypotheses 72:76-83.

Czigner A, Mihály A, Farkas O, Büki A, Krisztin-Péva B, Dobó E, Barzó P (2004) Dynamics and regional distribution of c-fos protein expression in rat brain after a closed head injury. Int J Mol Med 14:247-252.

Donat CK, Scott G, Gentleman SM, Sastre M (2017) Microglial Activation in Traumatic Brain Injury. Front Aging Neurosci 9:208.

Dougherty AL, MacGregor AJ, Han PP, Viirre E, Heltemes KJ, Galarneau MR (2013) Blast-related ear injuries among U.S. military personnel. J Rehabil Res Dev 50:893-904.

Dougherty AL, MacGregor AJ, Viirre E, Clouser MC, Han PP, Quinn KH, Galarneau MR (2018) Preliminary study of hearing protection and non-impact, blast-induced concussion in US military personnel. Brain Inj 32:1423-1428.

Ewert DL, Lu J, Li W, Du X, Floyd R, Kopke R (2012) Antioxidant treatment reduces blast-induced cochlear damage and hearing loss. Hear Res 285(1-2):29-39.

Fausti SA, Wilmington DJ, Gallun FJ, Walker WC, Cifu DX, Ochs AL, Lew HL (2009) Auditory and vestibular dysfunction associated with blast-related traumatic brain injury. J Rehabil Res Dev 46:797-810.

Gill J, Cashion A, Osier N, Arcurio L, Motamedi V, Dell KC, Carr W, Kim HS, Yun S, Walker P, Ahlers S, LoPresti M, Yarnell A (2017) Moderate blast exposure alters gene expression and levels of amyloid precursor protein. Neurol Genet 3:e186.

Guzman-Martinez L, Maccioni RB, Andrade V, Navarrete LP, Pastor MG, Ramos-Escobar N (2019) Neuroinflammation as a common feature of neurodegenerative disorders. Front Pharmacol 10:1008.

Hansen DV, Hanson JE, Sheng M (2018) Microglia in Alzheimer's disease. J Cell Biol 217:459-472.

Hicks RR, Fertig SJ, Desrocher RE, Koroshetz WJ, Pancrazio JJ (2010) Neurological effects of blast injury. J Trauma 68:1257-1263.

Kim JH, Goodrich JA, Situ R, Rapuano A, Hetherington H, Du F, Parks S, Taylor W, Westmoreland T, Ling G, Bandak FA, de Lanerolle NC (2020) Periventricular white matter alterations from explosive blast in a large animal model: mild traumatic brain injury or "subconcussive" injury? J Neuropathol Exp Neurol 79:605-617.

Kinney JW, Bemiller SM, Murtishaw AS, Leisgang AM, Salazar AM, Lamb BT (2018) Inflammation as a central mechanism in Alzheimer's disease. Alzheimers Dement (N Y) 4:575-590.

Leng F, Edison P (2020) Neuroinflammation and microglial activation in Alzheimer disease: where do we go from here? Nat Rev Neurol doi: 10.1038/s41582-020-00435-y.

Ma X, Aravind A, Pfister BJ, Chandra N, Haorah J (2019) Animal models of traumatic brain injury and assessment of injury severity. Mol Neurobiol 56:5332-5345.

Marciano PG, Eberwine JH, Ragupathi R, Saatman KE, Meaney DF, McIntosh TK (2002) Expression profiling following traumatic brain injury: a review. Neurochem Res 27:1147-1155.

Mediavilla Varas J, Philippens M, Meijer SR, van den Berg AC, Sibma PC, van Bree JL, de Vries DV (2011) Physics of IED blast shock tube simulations for mTBI research. Front Neurol 2:58.

Moss WC, King MJ, Blackman EG (2009) Skull flexure from blast waves: a mechanism for brain injury with implications for helmet design. Phys Rev Lett 103:108702.

Muelbl MJ, Slaker ML, Shah AS, Nawarawong NN, Gerndt CH, Budde MD, Stemper BD, Olsen CM (2018) Effects of mild blast traumatic brain injury on cognitive- and addiction-related behaviors. Sci Rep 8:9941.

Newman AJ, Hayes SH, Rao AS, Allman BL, Manohar S, Ding D, Stolzberg D, Lobarinas E, Mollendorf JC, Salvi R (2015) Low-cost blast wave generator for studies of hearing loss and brain injury: blast wave effects in closed spaces. J Neurosci Methods 242:82-92.

Olivera A, Lejbman N, Jeromin A, French LM, Kim HS, Cashion A, Mysliwiec V, Diaz-Arrastia R, Gill J (2015) Peripheral total tau in military personnel who sustain traumatic brain injuries during deployment. JAMA Neurol 72:1109-1116.

Penley SC, Gaudet CM, Threlkeld SW (2013) Use of an eight-arm radial water maze to assess working and reference memory following neonatal brain injury. J Vis Exp:50940.

Rusiecki J, Levin LI, Wang L, Byrne C, Krishnamurthy J, Chen L, Galdzicki Z, French LM (2020) Blast traumatic brain injury and serum inflammatory cytokines: a repeated measures case-control study among U.S. military service members. J Neuroinflammation 17:20.

Russell AL, Richardson MR, Bauman BM, Hernandez IM, Saperstein S, Handa RJ, Wu TJ (2018) Differential responses of the HPA axis to mild blast traumatic brain injury in male and female mice. Endocrinology 159:2363-2375.

Sandlin DS, Yu Y, Huang J, Zhang C, Arteaga AA, Lippincott JK, Peeden EOH, Guyton RR, Chen L, Beneke LLS, Allison JC, Zhu H, Zhou W (2018) Autonomic responses to blast overpressure can be elicited by exclusively exposing the ear in rats. J Otol 13:44-53.

Seibenhener ML, Wooten MC (2015) Use of the Open Field Maze to measure locomotor and anxiety-like behavior in mice. J Vis Exp:e52434.

Simard JM, Pampori A, Keledjian K, Tosun C, Schwartzbauer G, Ivanova S, Gerzanich V (2014) Exposure of the thorax to a sublethal blast wave causes a hydrodynamic pulse that leads to perivenular inflammation in the brain. J Neurotrauma 31:1292-1304.

Simon DW, McGeachy MJ, Bayır H, Clark RS, Loane DJ, Kochanek PM (2017) The far-reaching scope of neuroinflammation after traumatic brain injury. Nat Rev Neurol 13:171-191.

Walker WC, Franke LM, McDonald SD, Sima AP, Keyser-Marcus L (2015) Prevalence of mental health conditions after military blast exposure, their co-occurrence, and their relation to mild traumatic brain injury. Brain Inj 29:1581-1588.

Wang YP, Hameed MQ, Rakhade SN, Iglesias AH, Muller PA, Mou DL, Rotenberge A (2014) Hippocampal immediate early gene transcription in the rat fluid percussion traumatic brain injury model. Neuroreport 25:954-959.

Wofford KL, Loane DJ, Cullen DK (2019) Acute drivers of neuroinflammation in traumatic brain injury. Neural Regen Res 14:1481-1489.

Xydakis MS, Bebarta VS, Harrison CD, Conner JC, Grant GA, Robbins AS (2007) Tympanic-membrane perforation as a marker of concussive brain injury in Iraq. N Engl J Med 357:830-831.

Yang Y, Wang H, Hu J, Hu H (2018) Lateral habenula in the pathophysiology of depression. Curr Opin Neurobiol 48:90-96.

Yu Y, Huang J, Tang X, Allison J, Sandlin D, Ding D, Pang Y, Zhang C, Chen T, Yin N, Chen L, Mustain W, Zhou W, Zhu H (2020) Exposure to blast shock waves via the ear canal induces deficits in vestibular afferent function in rats. J Otol 15:77-85.

C-Editors: Zhao M, Li CH; T-Editor: Jia Y